Negative differential magnetization in ultrathin Fe on vicinal W(100)

Yugui Yao,[1,2] Hector C. Mireles,[1] Jie Liu,[1] Qian Niu,[1] and J. L. Erskine[1]
[1]*Department of Physics, University of Texas, Austin, Texas 78712*
[2]*ICQS and Institute of Physics, Chinese Academy of Sciences, Beijing 100080, China*
(Received 30 January 2003; published 15 May 2003)

Magnetic hysteresis loops produced by ultrathin Fe films grown on stepped W(100) surfaces exhibit a region of negative differential magnetization when switching between magnetically saturated states. This interesting effect is explained by theoretical simulations based on a model Hamiltonian that includes both cubic and in-plane uniaxial anisotropy, and incorporates antiferromagnetic coupling between nanodomains which may result from a special growth condition used in the experiment.

DOI: 10.1103/PhysRevB.67.174409 PACS number(s): 75.30.Gw, 78.20.Ls

I. INTRODUCTION

Magnetic thin films grown on vicinal surfaces exhibit a rich variety of hysteresis loops and thickness-dependent reorientation transitions as a result of interplay between surface and step induced anisotropies.[1–5] Néel's[6] pair-bonding model and its extensions[7] to specific epitaxial film systems [Fe/W(100) and Co/Cu(111)] account for the primary effects of surface and step anisotropy including the direction of preferred spin alignment and the step-density dependence of the switching fields.[3] Numerical simulations based on phenomenological uniform phase (single-domain) models[8] have produced hysteresis loops similar to ones observed on Fe/W(100), for instance, and have also provided phase diagrams relating the loop shapes to the anisotropy parameters of the model Hamiltonian. Other systems manifest radically different behavior. For example, Fe sesquilayers on vicinal W(110) (Refs. 9–12) grow via a step-flow mode that produces nanostripe arrays consisting of alternating monolayer/double layer (ML/DL) stripes. These two-phase structures manifest interesting magnetic behavior: a thickness-dependent reorientation transition driven by dipolar antiferromagnetic coupling between the DL nanodomains.

In this paper, we report observation of hysteresis loops for $p(1\times1)$ Fe films on vicinal W(100) that exhibit negative differential magnetization (NDM). The differential magnetic susceptibility at a segment of negative slope is two orders of magnitude larger than the total diamagnetism in the Meissner effect of superconductors. A negative slope beyond the Meissner limit implies a local thermodynamic instability of the magnetic state, and cannot be explained within uniform-phase models according to a general argument to be presented below. We show that a two-phase model with antiferromagnetic coupling can explain the instability, but that the coupling for Fe/W(100) does not appear to be dipolar as in the case of the stripe domain structure of Fe/W(110). While exchange-coupled magnetic switching leading to negative differential magnetization has been observed in multilayer thin film systems, our observation of this phenomenon in a single-material ultrathin epitaxial film system is unique. The model that we propose to explain this phenomenon is based on self-assembled structures formed at surface steps [similar to those that have been reported on W(110)] that support nanometer-scale coupled magnetic domains.

II. EXPERIMENT

Figure 1 displays hysteresis loops measured from 2.5-monolayer-thick $p(1\times1)$ Fe on vicinal W(100). The W(100) surface was cleaned *in situ* by repeated cycles of annealing in oxygen (1500 K/10^{-6} torr) followed by flashing to 2500 K. The Fe films were grown at $\sim$0.5 ML/min using an electron beam heated pendent-drop source at pressures below 5 $\times10^{-10}$ torr. The first ML was grown at a substrate temperature of 500 K; subsequent layers were grown at $\sim$300 K.

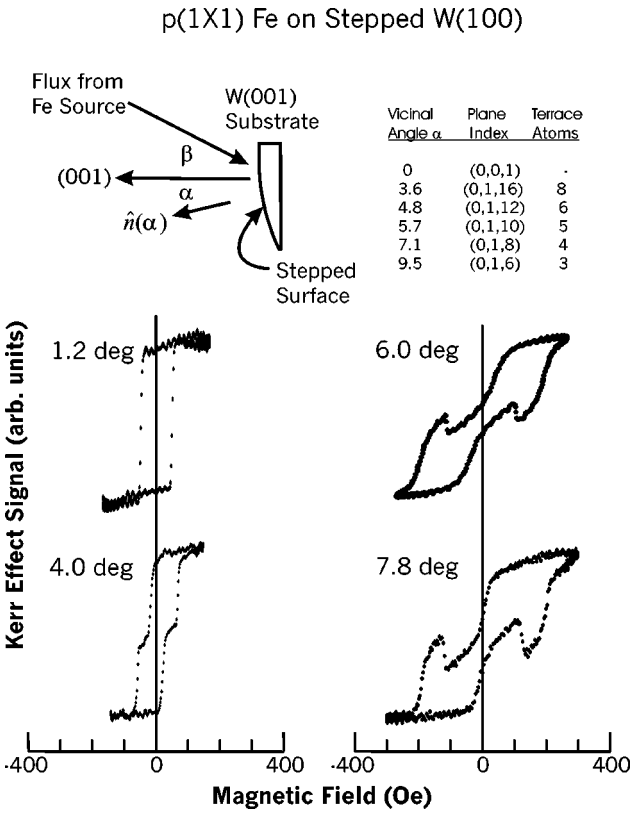

FIG. 1. Hysteresis loops measured using the longitudinal Kerr effect for 2.5-ML Fe films on a graded-step-density W(100) crystal. Insets show film growth geometry and plane index/terrace atom number dependence on vicinal angle α. Loop at $\alpha=4°$ does not exhibit strong step induced perpendicular anisotropy observed in prior experiments (Refs. 5 and 13) and loops for $\alpha\geqslant6$ exhibit negative differential magnetization.

The growth substrate and films were characterized using electron diffraction and Auger electron spectroscopy as described in prior publications.[1,5,13] The longitudinal magneto-optic Kerr effect with *s*-polarized light, focused to a 50-micrometer-diameter spot, was used to measure the hysteresis loops. The sinusoidal applied magnetic field (1 Hz) was parallel to the steps. The primary difference in film growth parameters in the present experiments (which appears to be responsible for the different behavior) was the orientation of the W(100) crystal in relation to the flux of Fe atoms ($\beta \sim 30°$) during film growth (Fig. 1). The intent was to use the asymmetry in growth geometry to affect the local atomic coordination along the step edges. According to the Néel pair-bonding model of step-induced anisotropy,[7] it is the atoms at the steps that govern the anisotropy; therefore the magnetic behavior should be very sensitive to minor changes in local atomic coordination at step edges.

The modified thin film growth geometry produces dramatic differences in hysteresis loop behavior at large vicinal angles. Loops measured at $\alpha = 0°$ and small vicinal angles are identical to loops measured in prior experiments.[1,3,5,13] At vicinal angles greater than 4°, however, major differences are apparent: in prior experiments (film grown with normal incidence flux) the step-induced anisotropy was observed to be very strong with a switching threshold at $H_s = -100$ Oe [Fig. 1(a), Ref. 13]; in Fig. 1 the switching threshold of the 4° vicinal angle film is $H_s = +25$ Oe. At 6.0° and 7.8° vicinal angles, the threshold is weakly negative, but nowhere near the threshold measured in prior experiments [Fig. 1(c) Ref. 13] $H_s = -300$ Oe at $\alpha = 7.1°$.

Even more dramatic is the NDM seen in the $\alpha = 6.0°$ and $\alpha = 7.8°$ loops. After reaching a local maximum as the the drive field is increased, the magnetization drops essentially to zero, over a small field interval, before turning up again. The differential magnetic susceptibility in this region can be estimated from the amount of drop relative to the saturation magnetization (which we assume to be similar to the bulk value) and from the width of the field interval. For the $\alpha = 7.8°$ case, this yields $dM/dH = -264$. This NDM effect is much larger than the so-called total diamagnetism in the Meissner effect of superconductors ($dM/dH = -1$).

The abrupt decrease in magnetization as a function of increasing field indicates a change of spin configuration that produces a new local minimum of free energy. Phenomenological models of magnetic anisotropy that allow out-of-plane magnetization[14] are capable of producing inverted loops and regions of weak NDM. However, we have not observed (by polar-Kerr effect experiments) any evidence of out-of-plane magnetization for 2–3-ML Fe on W(100). Therefore we believe that in-plane magnetization configurations are responsible for the different magnetic behavior shown in Fig. 1.

III. PHENOMENOLOGICAL MODEL

NDM cannot be produced by a uniform phase model of in-plane spins. The free energy of a magnetic system having cubic and in-plane uniaxial anisotropy subjected to an applied magnetic field h along the x axis can be written $E = f(M) - hM$ where f describes all anisotropy energies and $-hM$ is the Zeeman energy. It is clear that, as h increases from $-h_{\max}$ to $+h_{\max}$, the magnetization M, which minimizes the free energy, must change monotonically.

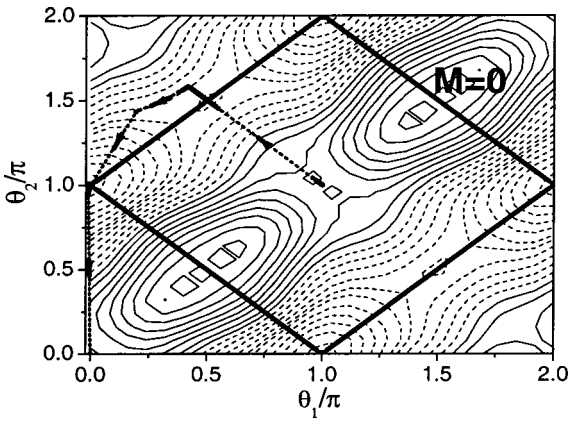

FIG. 2. Potential-energy contour plot at $h = 0$ for $K_2/K_4 = 3$ and $a/K_4 = 8$ as a function of θ_1 and θ_2 that describe nanodomain magnetization directions. Diamond shaped frame shows loci of θ_1, θ_2 corresponding to $M = 0$. Spin configuration trajectory (dotted line with arrows) corresponds to a hysteresis loop with two $M = 0$ configurations and a region of NDM.

Therefore we develop a two-phase model in which the system free energy is a function of two variables, θ_1 and θ_2 representing the spin orientation of adjacent magnetic nanodomains in relation to the applied magnetic field. This is also motivated by the fact that loops exhibiting NDM are observed in coupled multilayer stacks.[15] We postulate that the nanodomains in our system are bound by step edges as proposed to qualitatively understand double magnetic switching in the same thin-film system.[13] The assumption of coupled nanodomains is also consistent with the antiferromagnetic configurations observed in magnetic nanowires of the Fe/W(110) system.[9–12] However, in our system Fe/W(100), the coupling mechanism does not appear to be dipolar as explained later. The model Hamiltonian for the two phase system is

$$H = -h(\cos\theta_1 + \cos\theta_2) + a\cos(\theta_1 - \theta_2) - \frac{K_2}{2}(\cos 2\theta_1 + \cos 2\theta_2) - \frac{K_4}{2}(\cos 4\theta_1 + \cos 4\theta_2), \tag{1}$$

where K_2 and K_4 are twofold and fourfold anisotropy constants, and a is the coupling strength between the nanodomains. The field h is applied along the steps. The easy axis can be either along the steps ($K_2 > 0$) or perpendicular to them ($K_2 < 0$),[16] and the coupling is allowed to be ferromagnetic ($a < 0$) or antiferromagnetic ($a > 0$). A less general form of the above model has been extensively analyzed for the cases with $K_2 = 0$ or $K_4 = 0$.[17]

Before discussing the hysteresis loops and the anisotropy phase diagram associated with this model, we examine the free-energy landscape of the Hamiltonian. Figure 2 displays a two-dimensional contour plot of the Hamiltonian (for se-

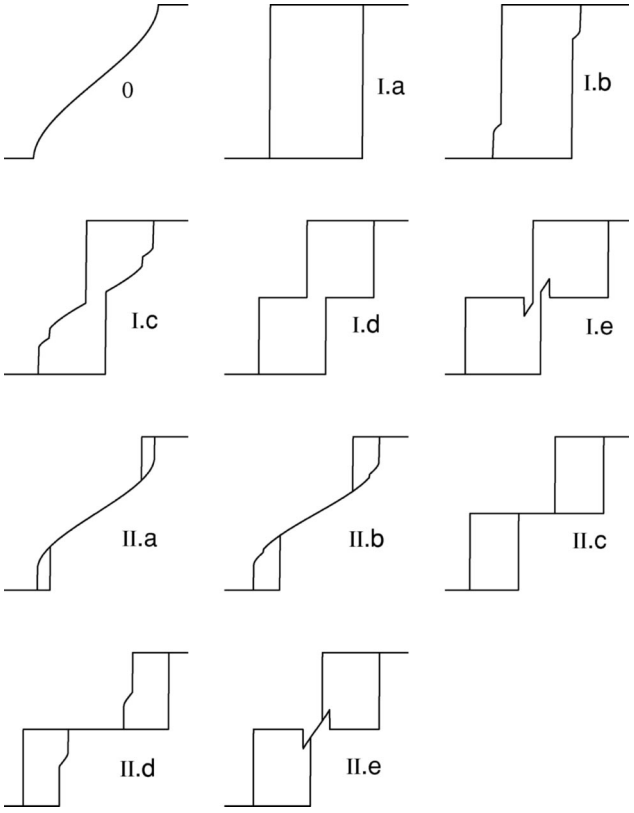

FIG. 3. Calculated hysteresis loops for various combinations of parameter a, K_2, and K_4. Loop topology designations O, I, II, and subvariants a, b, c, d, e correspond to regions of the anisotropy phase diagram displayed in Fig. 4.

lected a, K_2, K_4) as a function of variables θ_1 and θ_2 for zero applied field ($h=0$). Every allowed spin configuration is represented by a pair of coordinates (θ_1,θ_2) and the magnetization averaged over the two domains is given by $M=\frac{1}{2}(\cos\theta_1+\cos\theta_2)$. Specifically, (0,0) and (π,π) represent saturated magnetization states of opposite polarity, and the diamond-shaped frame represents the loci of θ_1, θ_2 combinations that yield $M=0$. The effect of an applied field h is to modify the $h=0$ contours by the Zeeman energy $-h(\cos\theta_1+\cos\theta_2)$, which drives the evolution of the magnetization state. The magnetization trajectory (dotted line with arrows), which will be discussed later, corresponds to specific values of K_2/K_4, and a/K_4 that produce NDM over a range of applied field h. Note that the trajectory describing the system spin configuration begins at $\theta_1=\theta_2=\pi$ (saturated state) and crosses the $M=0$ line twice before reaching the reversed magnetization state $\theta_1=\theta_2=0$. It is possible for the system to produce a second $M=0$ state without duplicating the spin configuration that produced a prior $M=0$ state.

Our numerical simulation starts with the initial saturation state $\theta_1=\theta_2=\pi$ for large negative h. The magnetization evolves to follow the local minimum of the free energy as h changes. Figure 3 displays a set of hysteresis loops generated by a series of simulations. The loops are categorized according to their topology: they can exhibit no hysteresis (loop O), a single loop (loops I) and double loops (loops II). The loops are further characterized by a, b, c, d, e to permit

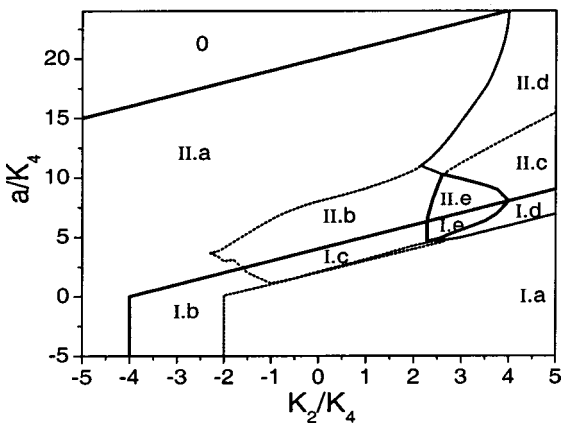

FIG. 4. Hysteresis loop phase diagram for model Hamiltonian Eq. (1). The parameter a describes the ferromagnetic ($a<0$) or antiferromagnetic ($a>0$) coupling between the two nanodomain phases, and K_2 describes the twofold anisotropy which favors($K_2<0$) perpendicular- or ($K_2>0$) parallel-to-step spin alignment. The parameters a and K_2 are normalized to K_4 the fourfold anisotropy constant. Regions I.e and II.e of the phase diagram produce loops that exhibit NDM.

identifying them with regions of the phase diagram shown in Fig. 4. The phase diagram displays specific regions of anisotropy and coupling parameters that produce the various hysteresis loops. The axes of Fig. 4 are the interdomain coupling strength a and the uniaxial anisotropy strength K_2, both scaled by the four-fold anisotropy constant K_4. Solid lines in Fig. 4 delineate major loop topologies, dotted lines divide phases into some subvariants.

With ferromagnetic coupling ($a<0$), our model reproduces the uniform-phase results of prior work.[8] With antiferromagnetic coupling ($a>0$), a number of new phases are produced. The spin configurations corresponding to various regions of the anisotropy phase diagram can be understood as follows: Region O: spins in the two nanodomains rotate reversibly and continuously according to $\theta_1=-\theta_2$; the free-energy contour plots do not develop saddle points that can produce ''jump'' behavior apparent in loops from other regions of the hysteresis loop phase diagram. The condition $2K_2+8K_4-2a=0$ defines the separation between phases I and II. Note that phases I.a, I.b, II.a, and O have been observed in the uniform single-domain model.[8] In this case K_2 was restricted to $K_2<0$ corresponding to the experimentally observed uniaxial anisotropy in 2-ML Fe on W(100) perpendicular to the steps. It is not surprising that these phases can also be produced in a two phase model with $K_2>0$ which also allows antiferromagnetic coupling because if $\theta_1=-\theta_2$ (typical for antiferromagnetic coupling) the coupling form becomes $a\cos(\theta_1-\theta_2)=a\cos(2\theta_1)$ which is equivalent to uniaxial anisotropy perpendicular to the steps in the single phase model.

The $\langle M\rangle=0$ state $(0,\pi)$ exists in phases I.e, I.d, II.c, II.d, and II.e, but does not exist in phases O, I.a, I.b, I.c, II.a, and II.b. We designate the former set of phases antiferromagnetic phases because a range of solutions in the drive-field-dependent $\langle M\rangle$ evolves between states (π,π) and (0,0) including the $\langle M\rangle=0$ state $(0,\pi)$. It is the combined effect of

a suitably strong antiferromagnetic coupling ($a/K_4 \sim 7$) and positive K_2 ($K_2/K_4 \sim 3$) that produce the potential contours required for negative differential magnetization in the two-phase model. Referring to Fig. 2, one can envision the evolution in spin configuration space of the free-energy contours as h varies from large negative to large positive values. The evolution of $\langle M \rangle$ (dotted path with arrows) is governed by the evolution of the local minima of the free energy. The point at which dM/dh becomes negative (regions I.e and II.e) can be solved for analytically yielding (M_d, h_d): i.e.,

$$M_d^2 = (28K_4 - a - K_2 - \sqrt{a^2 + 2a(K_2 - 28K_4) + (K_2 + 20K_4)^2})/(48K_4),$$

$$h_d = (2a - 2K_2)M_d + 8K_4(1 - 2M_d^2)M_d .$$

M_d and h_d increase when the coupling strength $a/K4$ increases and the anisotropy K_2/K_4 decreases. Competition between a and K_2 in the region near (h_d,M_d) produce a potential-energy landscape that results in negative differential magnetization as h is varied.

Measured hysteresis loops from ultrathin Fe on W(100) suggest that many of the regions of the phase diagram (Fig. 4) are accessible by suitable choice of sample preparation parameters. Step-density-dependent studies[1,3,5] of 2-ML $p(1\times1)$ Fe on W(100) suggest that loops from this system progress from I.a to I.b to II.a of Fig. 4 (IV to III to II of Ref. 8), consistent with $a<0$, $K_2<0$, and K_2 becoming more negative as α is increased. However, the evolution of loop shape in Fig. 1 suggest a progression of hysteresis behavior from I.a to I.d to I.e in Fig. 4; this requires $a>0$ and $K_2>0$ for the 2.5-ML Fe on W(100) grown at an oblique angle. Thus some combination of film thickness and growth geometry results in a different in-plane anisotropy.

IV. DISCUSSION

Important questions are open regarding the origin of antiferromagnetic coupling and parallel-step anisotropy, which are required to explain the experimental data. The required parallel to-steps in-plane anisotropy is compatible with Néel model predictions[7] of a thickness-dependent in-plane reorientation transition at about 3.5 ML's in which the easy direction changes from perpendicular to parallel to step edges [although such a transition has not been confirmed by direct experimental observation for Fe on W(100)]. Also, the loops (Fig. 1) at low vicinal angle (4.0°) do not exhibit the striking switching to $\langle M \rangle = 0$ at negative H associated with strong perpendicular-to-step in-plane anisotropy. Thus, the required anisotropy is not unreasonable. For the present system, as we postulated before, shadowing effects or other effects resulting from the different growth geometry (with off-normal flux) may weaken the magnetic coupling across the step edges, forming one-dimensional domains defined by the terraces. These terrace domains may be interrupted in the longitudinal direction by thermal fluctuations, but their coherence lengths are expected to be much longer than the terrace width. We calculated the energy of dipolar interactions between the Fe moments within such a domain, and found its anisotropy form in perfect agreement with the K_2 term in Eq. (1). For a domain of monolayer thickness, $K_2 = +2.5 \times 10^{-2}$ erg/cm^2 for a four-atom wide strip and $K_2 = +1.8 \times 10^{-2}$ erg/cm^2 for a six-atom wide strip. The positive signs indicate an easy direction parallel to the steps, satisfying our requirement for producing NDM. Quantitatively, if K_4 adopts the typical value $\sim 10^{-2}$ erg/cm^2 for a flat film,[8] we find that our parameter K_2/K_4 is also not far from the range required. On the other hand, dipolar interaction between the domains cannot produce antiferromagnetic coupling when the spins are fixed in the plane. This is in contrast with the case of Refs. 9–12, where spins are perpendicular to the surface. It is possible that nonmagnetic gaps may exist between the domains due to the different growth procedure, and indirect exchange interaction mediated by the gap regions can be antiferromagnetic, just as magnetic layer stacks may be antiferromagnetically coupled through nonmagnetic spacers.[18] Further experimental work is needed to confirm this point; scanning tunneling microscope capability would be very useful in resolving the structural features of this system.

V. CONCLUSIONS

We have observed NDM accompanied by two $M=0$ states in hysteresis loops produced by thin Fe films on vicinal W(100). This interesting behavior is explained by a two-phase model that incorporates in-plane antiferromagnetic coupling between step-governed nanodomains. The antiferromagnetic coupling appears to originate from an exchange rather than dipolar mechanism. With this nondipolar mechanism, the different phenomena we have reported can be viewed as a single-film analog of the multilayer stack coupling through nonmagnetic layers that is finding application in GMR and other device structures.

ACKNOWLEDGMENTS

This work was supported by NSF Contract No. DMR-9972113, DoE DE-FG03-02ER45958, and the R. A. Welch Foundation. We acknowledge useful discussions with Z. Q. Qiu.

[1] J. Chen and J. L. Erskine, Phys. Rev. Lett. **68**, 1212 (1992).

[2] A. Berger, U. Linke, and H. P. Oepen, Phys. Rev. Lett. **68**, 839 (1992).

[3] R. K. Kawakami, E. J. Escorcia-Aparicio, and Z. Q. Qiu, Phys. Rev. Lett. **77**, 2570 (1996); H. J. Choi, Z. Q. Qiu, J. Pearson, J. S. Jiang, D. Li, and S. D. Bader, Phys. Rev. B **57**, R12 713 (1998).

[4] T. Leeb, M. Brockmann, F. Bensch, S. Miethaner, and G. Bayreuther, J. Appl. Phys. **85**, 4964 (1998).

[5] H. C. Mireles and J. L. Erskine, J. Appl. Phys. **89**, 6671 (2001).

[6] L. Néel, J. Phys. Radium **15**, 225 (1954).
[7] D. S. Chuang, C. A. Ballentine, and R. C. O'Handley, Phys. Rev. B **49**, 15084 (1994).
[8] R. A. Hyman, A. Zangwill, and M. D. Stiles, Phys. Rev. B **58**, 9276 (1998), and references therein.
[9] J. Hauschild, U. Gradmann, and H. J. Elmers, Appl. Phys. Lett. **72**, 3211 (1998).
[10] H. J. Elmers, J. Hauschild, and U. Gradmann, Phys. Rev. B **59**, 3688 (1999).
[11] O. Pietzsch, A. Kubetzka, M. Bode, and R. Wiesendanger, Phys. Rev. Lett. **84**, 5212 (2000).
[12] M. Bode, O. Pietzsch, A. Kubetzka, S. Heinze, and R. Wiesendanger, Phys. Rev. Lett. **86**, 2142 (2001).
[13] H. C. Mireles and J. L. Erskine, Phys. Rev. Lett. **87**, 037201 (2001).
[14] M. Cougo dos Santos, J. Geshev, J. E. Schmidt, S. R. Teixeira, and L. G. Pereira, Phys. Rev. B **61**, 1311 (2000).
[15] D. Pescia and P. Grünberg, IFF Bulletin **33**, 3 (1988).
[16] K_2 in this phenomenological model could include a contribution from the dipolar mechanism, see R. Arias and D. L. Mills, Phys. Rev. B **59**, 11871 (2000).
[17] B. Dieny and J. P. Gavigan, J. Phys.: Condens. Matter **2**, 187 (1990).
[18] P. Grünberg, R. Schreiber, Y. Pang, M. B. Brodsky, and H. Sowers, Phys. Rev. Lett. **57**, 2442 (1986).